

1 **Anthropogenic modification of phosphorus sequestration in lake**
2 **sediments during the Holocene: A global perspective**

3 Luyao Tu ^{a, b}, Madeleine Moyle ^c, John F. Boyle ^c, Paul D. Zander ^d, Tao Huang ^e, Lize
4 Meng ^e, Changchun Huang ^{e, *}, Xin Zhou ^{f, *}, Martin Grosjean ^b

5 ^a Department of Marine Science and Engineering, Nanjing Normal University, Nanjing
6 210023, China

7 ^b Oeschger Centre for Climate Change Research & Institute of Geography, University of
8 Bern, Bern 3012, Switzerland

9 ^c Department of Geography and Planning, University of Liverpool, Liverpool L69 3BX,
10 United Kingdom

11 ^d Climate Geochemistry Department, Max Planck Institute for Chemistry, Mainz 55128,
12 Germany

13 ^e Department of Geography Science, Nanjing Normal University, Nanjing 210023, China

14 ^f Department of Earth and Space Sciences, University of Science and Technology of China,
15 Hefei 230026, China

16 Correspondence author: Xin Zhou (xinzhou@ustc.edu.cn) & Changchun Huang
17 (huangchangchun@njnu.edu.cn)

18

19 **Abstract**

20 Human activity has fundamentally altered the global phosphorus (P) cycle. Yet our
21 understanding of when and how humans influenced the P cycle has been limited
22 by the scarcity of long-term P sequestration records, particularly outside Europe
23 and North America. Lake sediments provide a unique archive of past P burial rates
24 and allow the human-mediated disruption of the global P cycle to be examined.
25 We compiled the first global-scale and continentally resolved reconstruction of
26 lake-wide Holocene P burial rates using 108 lakes from around the world. In
27 Europe, lake P burial rates started to increase noticeably after ~4000 calendar
28 years before 1950 CE (cal BP), whereas the increase occurred later in China

29 (~2000 cal BP) and in North America (~550 cal BP), which is most likely related to
30 different histories of population growth, land-use and associated soil erosion
31 intensities. Anthropogenic soil erosion explains ~86% of the observed changes in
32 global lake P burial rates in pre-industrial times. We also provide the first long-term
33 estimates of the global lake P sink over the Holocene (~2686 Tg P). We estimate
34 that the global mean lake sediment P sequestration since 1850 CE (100 cal BP) is
35 ~1.54 Tg P yr⁻¹, representing approximately a six-fold increase above the mean
36 pre-industrial value (~0.24 Tg P yr⁻¹; 11,500 to 100 cal BP) and around a ten-fold
37 increase above the Early-Middle Holocene low-disturbance baseline of 0.16 Tg P
38 yr⁻¹. This study suggests that human activities have been affecting the global P
39 cycle for millennia, with substantial alteration after industrial times (1850 CE).

40 **Key words:** Phosphorus; Lake sediments; Holocene; Human impacts; Land use

41

42 **1. Introduction**

43 Phosphorus (P) is an essential element for life on Earth and is a critical nutrient for
44 plant growth and food production (Cordell et al., 2009; Alewell et al., 2020). Recent
45 human activities have substantially altered the global terrestrial P cycle (Ashley et
46 al., 2011; Chen et al., 2016; Yuan et al., 2018), and a safe planetary boundary for
47 P has been exceeded (Steffen et al., 2015), risking future food production (Alewell
48 et al., 2020). Furthermore, the resulting excessive anthropogenic P loading to
49 global freshwaters has exacerbated lake eutrophication, negatively affecting
50 biodiversity and health of aquatic ecosystems (Smil, 2000; Jenny et al., 2019).
51 Although it is not known when the Earth shifted from nature-dominated to human-
52 dominated, inferring pre-disturbance P processes is critical to understanding the
53 trajectory of the global P cycle over centennial to multi-millennial timescales.

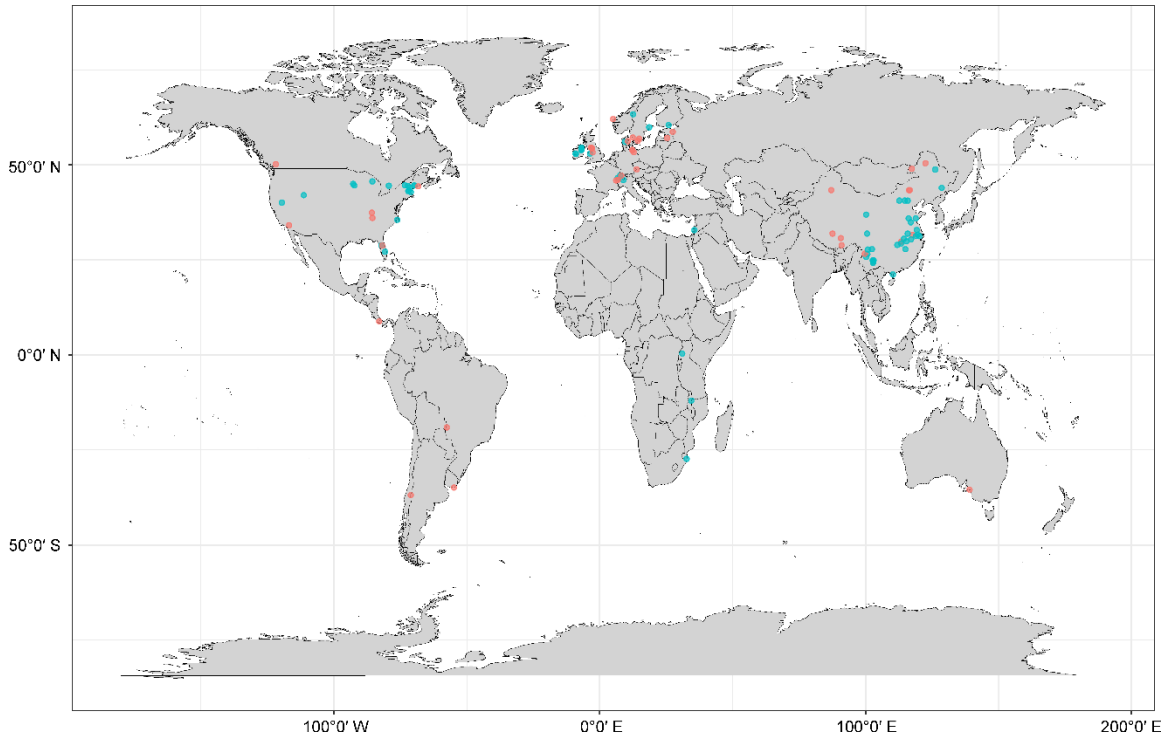
54 Lake sediment cores are valuable archives for assessing temporal dynamics of
55 terrestrial P cycling because of the strong linkage between catchment P loading
56 and sediment P burial (Boyle, 2002; Moyle et al., 2021a; Moyle and Boyle, 2021).
57 Therefore, records of P accumulation in sediments provide estimates of the timing,
58 magnitude, and extent of anthropogenic disturbance to catchment-scale P cycles.

59 Characterizing the temporal variability of lake P burial rates across broad
60 geographic areas is critical for understanding the global P cycle (Anderson et al.,
61 2020). Although anthropogenic drivers of changes in sediment P records have
62 been investigated intensively, most studies have focused on limited spatial scales
63 (individual lakes) or relatively short time periods (typically the last one or two
64 centuries) (Wang et al., 2021; Bhattacharya et al., 2022). Furthermore, most
65 relevant publications report only sediment P concentrations instead of basin-wide
66 P burial rates. Sediment P accumulation rates from single cores are likely to be
67 biased by sediment focusing in the lake (Scholtysik et al., 2022) and, thus, may
68 not represent the pattern of lake-wide mean sediment P sequestration. Previous
69 studies of long-term P burial largely focused on North America and Europe (Moyle
70 et al., 2021a), which highlights gaps in a global coverage of P records. This is
71 particularly true for China, which has a long history of agricultural P use (Ashley et
72 al., 2011). Several studies have shown that early anthropogenic deforestation and
73 farming in Europe started to have detectable impacts on lake P burial rates and P
74 cycle millennia ago (Boyle et al., 2015; Klamt et al., 2021; Moyle et al., 2021a),
75 and similar patterns are likely for lake sediments in China.

76 To date, a truly global synthesis of lake P records on centennial to millennial
77 timescales is missing, and there is also a lack of a well-constrained and long-term
78 global estimate of total lake P sequestration. In this study, we substantially extend
79 an existing meta-analysis of Holocene lake-sediment P burial (Moyle et al., 2021a),
80 presenting records from 108 lakes on six continents (Fig. 1). This dataset
81 represents the largest and most widely distributed coverage of lake-wide P burial
82 rates so far. We explore patterns of lake P burial rates during the Holocene at
83 global and continental scales and relate these to early and recent anthropogenic
84 disturbances (e.g., land use, soil erosion, P fertilizer inputs, and sewage disposal).

85 Furthermore, for the first time we produce a global estimate of lake P sequestration
86 throughout the Holocene and propose incorporating this long-term record into
87 Earth System Models (ESMs).

88



89

90 Fig. 1. Global distribution of sediment P records from 108 lakes in the study. The pink
 91 color indicates lakes with long-term P records (> 200 years) and the blue color with more
 92 recent P records (since 1850 CE).

93 2. Materials and methods

94 2.1. Data synthesis

95 Our database consists of sediment-P data from 108 lakes in North America,
 96 Europe, China, West Asia, Africa, South America, and Australia and were derived
 97 from published sources (Fig. 1; Supplementary Table S1). The five critical criteria
 98 during the site-selection process were the availability of (i) chronologies (AMS ^{14}C
 99 dates for records longer than 200 years and ^{210}Pb and /or ^{137}Cs data for records
 100 less than 200 years), (ii) P concentrations or P burial rates in sediment cores, (iii)
 101 location of the lake, (iv) mean water depth of the lake, and (v) water depth of the
 102 coring site. The largest number of lakes in this study is from China (41), followed
 103 by Europe (34), North America (25), South Africa (3), South America (3), West
 104 Asia (1), and Australia (1). Recalibration of existing ^{14}C ages was performed using
 105 OxCal 4.0 (Ramsey, 2009). Calibration of ^{14}C ages in lakes of the Northern

106 Hemisphere was performed using the IntCal20 calibration curve (cal BP, 2σ
107 probability, Reimer et al., 2020). The Southern Hemisphere calibration curve
108 SHCal04 (McCormac et al., 2004) was used for ^{14}C ages of lakes in the Southern
109 Hemisphere. Short P records (covering the past 100–200 years) were from North
110 America, Europe, China, and Africa, and long P records (covering time periods
111 longer than the past 200 years) were from North America, Europe, China, South
112 America, and Australia. Although the total dataset does not include all studies of
113 lake sediment P undertaken to date, it represents the largest and the longest
114 temporal synthesis of lake P burial rates to date.

115 2.2. Sediment-inferred mean lake-wide P burial rates

116 A simple process model (Moyle and Boyle, 2021) was applied to published
117 records of sediment-core P concentrations or sediment-core P burial rates to
118 calculate sediment-inferred mean lake-wide P burial rates (L_{sed} ; $\text{m}^{-2} \text{yr}^{-1}$) for the
119 Holocene (i.e., the last 11,500 calendar years before present, where present is
120 defined as 1950 CE). L_{sed} considers sediment focusing effects within a lake basin,
121 and for this study we assume that sediment focusing intensity remains constant
122 through a lake's history. As L_{sed} represents the lake-wide mean P burial rate, it
123 enables comparison of P records between different sites (Moyle and Boyle, 2021;
124 Moyle et al., 2021a). For the purpose of this study, the P retention coefficient,
125 defined as the proportion of P supplied that is retained in the lake sediments, was
126 not considered mainly because these values are not generally available for most
127 of the lakes. Also, according to Moyle et al. (2021a), temporal changes in lake P
128 retention coefficients during the Holocene are relatively small compared with
129 between-site differences. Therefore, P net sequestration rates in most of our
130 sediment records can still provide reliable information about long-term variation of
131 P loading from the catchment to lakes.

132 In our dataset, Holocene records of L_{sed} for 24 lakes in North America and Europe
133 (Table S1) were collected from the database of Moyle et al. (2021b). For other
134 lakes, L_{sed} was calculated using the equations in Moyle and Boyle (2021): L_{sed}
135 = $L_{\text{core}} \times Z_{\text{mean}} / Z_{\text{core}}$; where L_{core} = P burial rate of the sediment core ($\text{mg m}^{-2} \text{yr}^{-1}$);

136 L_{core} is calculated based on sediment P concentrations (P_{con} , $mg\ g^{-1}$) and core
137 mass accumulation rates (MAR, $g\ m^{-2}\ yr^{-1}$) given by: $L_{core} = P_{con} \times MAR$; Z_{mean} =
138 mean water depth of the lake (m); Z_{core} = water depth of the coring site (m). If MAR
139 was not reported in the original publications, it was calculated based on sediment
140 accumulation rates (SAR, $cm\ yr^{-1}$) from the age-depth model and the dry bulk
141 density (DBD, $g\ cm^{-3}$) of the sediment core, as given by: $MAR = SAR \times DBD \times 10^4$.
142 In studies for which DBD was not available, it can be estimated reliably by the
143 following methods:

144 1) Water contents (W , g/g) of sediments were preferentially used. In cases for
145 which W was reported, DBD is given by Moyle and Boyle (2021):

$$146\ DBD = (1-W) / (W/d_w + (1-W)/d)$$

147 Where d_w = Water Density, taken as $1.0\ g\ cm^{-3}$, and d = Minerogenic Sediment
148 Density, taken as $2.7\ g\ cm^{-3}$.

149 2) If water contents were not reported but loss on ignition (LOI, wt.%; at $550^\circ C$) for
150 the core sediment was reported, DBD is given by Moyle and Boyle (2021):

$$151\ DBD = 2.13 \times LOI^{-0.682}$$

152 3) If neither water contents nor LOI were reported but total organic carbon (TOC,
153 wt.%) data were available, DBD is estimated based on the following formula
154 (Avnimelech et al., 2001):

$$155\ DBD = 1.665 \times (TOC)^{-0.887} \quad (TOC > 6\%)$$

$$156\ DBD = 1.776 - 0.363 \times \ln(10 \times TOC) \quad (TOC \leq 6\%).$$

157 For the site-specific geochemical parameters used to apply the model, refer to
158 Table S1.

159 2.3. Estimation of global lake P burial rates using biomes

160 Following the approach of Anderson et al. (2020), we used global biomes as a
161 basis for identifying coherent landscape types and to scale up L_{sed} from individual
162 lake records to the global estimate of Holocene P sequestration. Firstly, the 108
163 lakes were assigned to global biomes based on their locations within The Nature

164 Conservancy's Terrestrial Ecoregion polygons, following Olson et al. (2001). Then,
165 the median of Lsed in each biome for three time-intervals (Early and Middle
166 Holocene 11,500-4000 cal BP, Late Holocene before pre-industrial times 4000-
167 100 cal BP, and modern times since 100 cal BP) was multiplied by lake areas from
168 the biome, following Anderson et al. (2020) in which the known area of the world's
169 22 largest lakes and the global reservoir lake areas are not considered. We
170 calculated global average Lsed as the sum of Lsed from all biomes. Although the
171 distribution of the 108 lakes across the different biomes is not homogenous, the
172 dataset over the last 11,500 years covers the majority (11 of 15) of the global
173 biomes (Fig. S1).

174 2.4. Statistical analysis

175 The statistical analysis was performed using R software (R CoreTeam, 2021). To
176 get matching ages to sediment P data, other records (e.g., SAR, MAR, DBD, LOI,
177 TOC, and W data) were interpolated in R using `approxfun` (method = "linear") in
178 "stats" package. The Lsed data were \log_{10} transformed prior to smoothed-trend
179 analyses to better represent the overall change patterns. Then, the trends of \log_{10}
180 (Lsed) were determined by fitting a simple generalized additive model (GAM) via
181 `gam()` function from the "mgcv" package (Wood, 2017) with REML smoothness
182 selection (using method = "REML") and the number of basis functions (k), following
183 the approach in Simpson (2018). We tested the number of basis functions (k)
184 required for the GAM models to sufficiently estimate the fitted trends.

185 Mean and median values of Lsed were calculated for each of the 100-year bins to
186 reflect the variation of Lsed at centennial scales during the Holocene. In a similar
187 way, mean and median values of Lsed were calculated for each of the 20-year
188 bins from 1850 CE to 2010 CE and the 10-year bins from 2010 CE to 2020 CE.
189 The breakpoints were detected on the mean curves of the 100-year bins for global
190 and continental data using the R package "BreakPoints" (Hurtado et al., 2020).

191 A GAM was applied to estimate the long-term impact of climate change (using
192 records of global temperature anomalies (MarcFott et al., 2013) and atmospheric
193 CO₂) and anthropogenic land-use disturbance (using records of global soil erosion

194 as indicated by SAR (Waters et al., 2016) and global cropland areas (Mottl et al.,
195 2021)) on the global Lsed values. The R package “mgcv” (Wood, 2017) was used
196 for calculating the GAM. The dataset for the GAM was calculated from the binned
197 mean values of every 100-year interval during the Holocene. We found a heavy
198 leverage of the data point at 50 cal BP (0-100 cal BP range) with the highest P
199 value and cropland area. Therefore, the time window between 11,450 and 100 cal
200 BP was selected for the modelling. The GAM formula to assess controls on Lsed
201 is a function of changes in SAR, global cropland areas (Cropland), global
202 temperature anomalies (Temp), and atmospheric CO₂ during the Holocene: $Lsed$
203 $\sim s(SAR) + s(Cropland) + s(Temp) + s(CO_2)$. P-value results are informative about
204 the contribution of SAR, Cropland, temperature, and atmospheric CO₂ to Lsed.

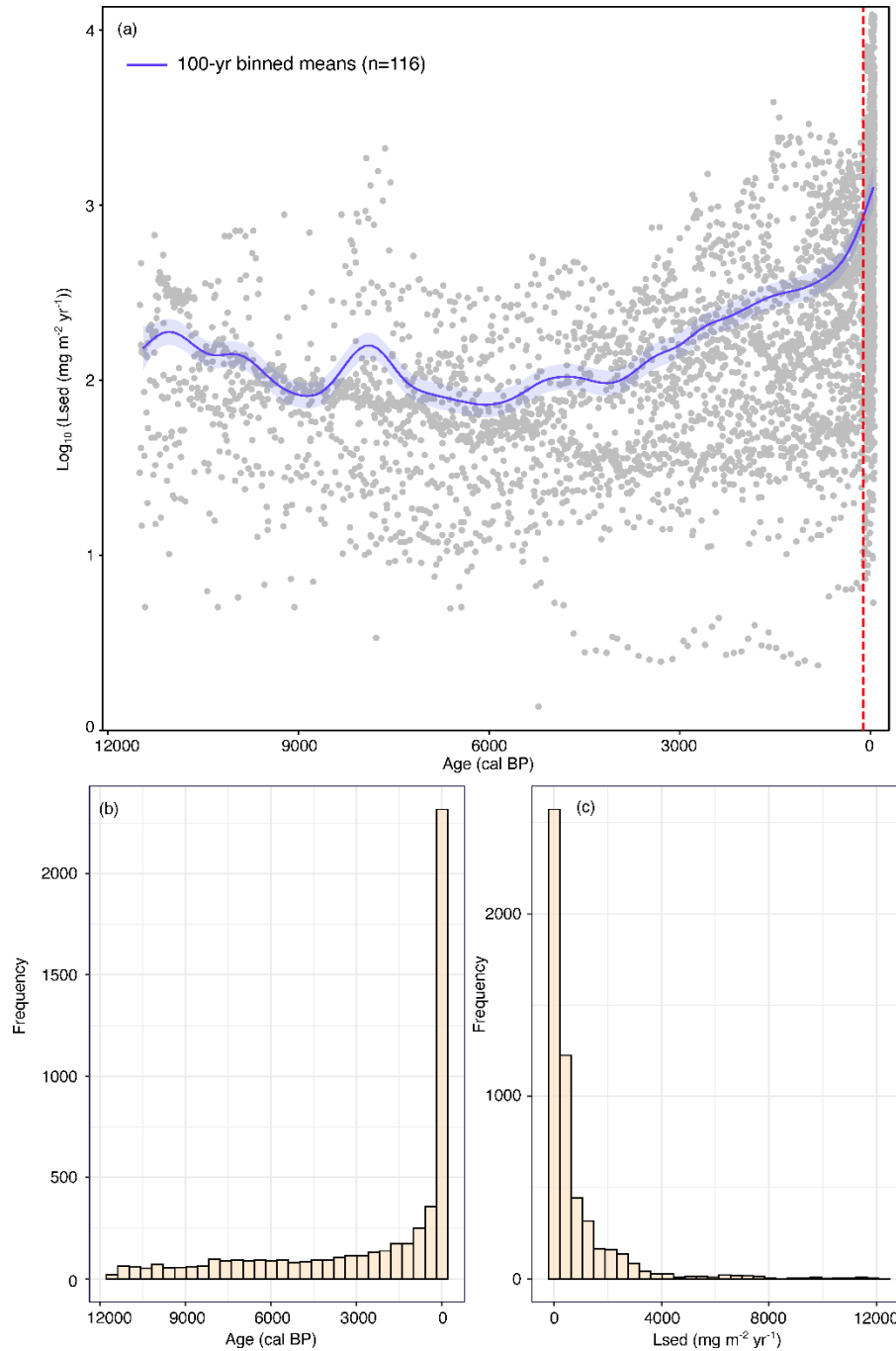
205 **3. Results and discussion**

206 3.1. Changes in lake P burial rates during the Holocene

207 Despite differences among continents, global and continental trajectories during
208 the Holocene show a similar pattern: the Lsed records all show unprecedented
209 high values after ~100 cal BP (after ~1850 CE; Fig. 2a; Fig. 3). This global-scale
210 pattern is consistent with the mean breakpoint year at 1900 CE (range 1850-1950
211 CE) in the global Lsed synthesis (Supplementary Fig. S2), which coincides with
212 recent definitions of the Anthropocene (Waters et al., 2016). In the last 100 to 200
213 years, intensive farming practices and industrialization have caused notable land-
214 use changes, which are responsible for intensified global soil erosion, P leaching
215 from agricultural soils, and P accumulation in lakes (Ruttenberg, 2003; Klein and
216 Ramankutty, 2004; Kemp et al., 2020; Zhang et al., 2022). The sharp increases in
217 Lsed values globally and continentally in the past 100–200 years (Fig. 2a; Fig.3)
218 undoubtedly were related to anthropogenic P transport from terrestrial to aquatic
219 systems (Yuan et al., 2018) via fertilizer use, P loss from agricultural systems via
220 soil erosion, and P discharge from sewage effluents . We estimate that the mean
221 global lake P burial rate since 1850 CE (100 cal BP) was $\sim 1.54 \text{ Tg P yr}^{-1}$ (Table
222 S2), representing a \sim six-fold increase above the mean pre-industrial value (~ 0.24
223 Tg P yr^{-1} ; 11,500 to 100 cal BP). As such, our results suggest that because of

224 unprecedented anthropogenic activities around the globe during the past 100-200
225 years, a fundamental shift in the global P cycle occurred, consistent with previous
226 studies (Yuan et al., 2018; Alewell et al., 2020).

227

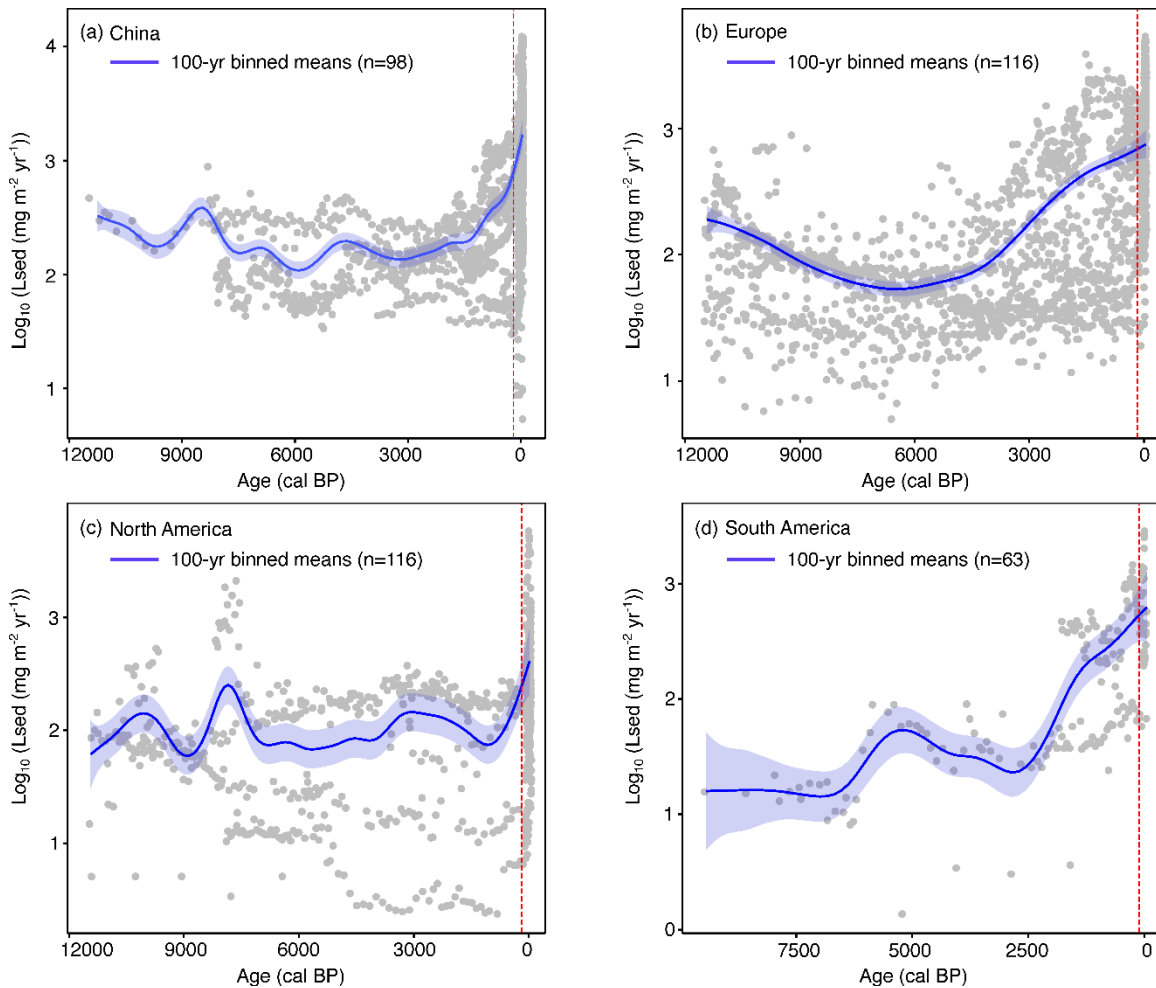


228

229 Fig. 2. (a) Generalized additive model (GAM) based trends fitted to the means of P data
230 in 100-yr bins (blue curve, basis dimension $k=30$, samples $n=116$) in 108 lakes during the

231 Holocene, with 95% confidence intervals on the predicted means (blue shaded envelopes);
 232 the blue fit is the result of a GAM with restricted maximum likelihood (REML) smoothness
 233 selection; the data of Lsed (shown as grey points) were \log_{10} transformed. The vertical
 234 dashed red line represents the breakpoint at 50 cal BP (i.e., mean breakpoint year,
 235 minimum-maximum range 0-100 cal BP). (b) Histogram (bins = 30) showing the frequency
 236 of 5365 calibrated ^{14}C ages. (c) Histogram (bins = 30) showing the frequency
 237 of Lsed.

238



239

240 Fig. 3. Generalized additive model (GAM) based trends fitted to the means of P data in
 241 100-yr bins (blue curves) from lakes in (a) China, (b) Europe, (c) North America, and (d)
 242 South America during the Holocene, with 95% confidence intervals on the predicted
 243 means (blue shaded envelopes); the blue fits are the results of a GAM with restricted
 244 maximum likelihood (REML) smoothness selection (basis dimension $k=30$). The vertical

245 dashed red line represents the breakpoint at 50 cal BP (i.e., mean breakpoint year,
246 minimum-maximum range 0-100 cal BP) for each continent; the data of Lsed (shown as
247 grey points) were \log_{10} transformed.

248 In the Early Holocene, Lsed records for the global average, China, Europe, and
249 North America all show relatively high values followed by decreasing trends
250 towards the Middle Holocene (Fig. 2a; Fig. 3a-c). This phenomenon can be mostly
251 explained by elevated catchment P supply from base-rich rejuvenated soils after
252 deglaciation in the Early Holocene, which was mainly attributed to natural soil
253 evolution driven by climate amelioration rather than human activities. Boyle et al.
254 (2013), Boyle et al. (2015) and Moyle et al. (2021a) also found high soil P export
255 associated with recently deglaciated landscapes. For P records of China, the
256 declining trend from the Early Holocene (11,500-8000 cal BP) to the Middle and
257 Late Holocene (Fig. 3a) mirrors the changes in soil erosion intensity in China (Fig.
258 4a) that were controlled predominantly by the Asian summer monsoon (Zhang et
259 al., 2022). In South America, limited data points in the Early and Middle Holocene
260 (~9500-5000 cal BP; n=25; Fig. 3d) result in large uncertainties and thus the
261 pattern is not discussed.

262 Although lake P burial rates among different continents all show maximal values
263 in the modern period compared to the last 11,500 years, there are notable
264 differences in the pre-industrial (before ~1850 CE) temporal evolution of P records
265 (Fig. 3). The most obvious difference is in the timing of the first visible increase in
266 P records. For instance, the P curve for European lakes began to increase
267 substantially after the onset of the Late Holocene around 4500-4000 years ago
268 (beginning of the Bronze Age in Europe; Fig. 3b). However, the first increases were
269 later in China (~2000 cal BP) and North America (~550 cal BP) (Fig. 3). In
270 landscapes that experienced early deforestation and farming, anthropogenic
271 landscape disturbance enhanced catchment P yield and sediment P sequestration
272 in lakes during the Middle and Late Holocene (Boyle et al., 2015; Klamt et al.,
273 2021). This is because P loss through catchment soil erosion was the dominant
274 contributor to lake P inputs (Carpenter et al., 1998; Yuan et al., 2018; Alewell et
275 al., 2020). During the Middle and Late Holocene, Lsed records for the global

276 average, Europe, and North America showed patterns consistent with their
277 respective anthropogenic soil erosion time-series (Fig. 4a). This indicates that the
278 different patterns of enhanced Lsed in the Late Holocene among these continents
279 are most likely attributed to differing soil erosion intensities associated with distinct
280 continental land use histories.

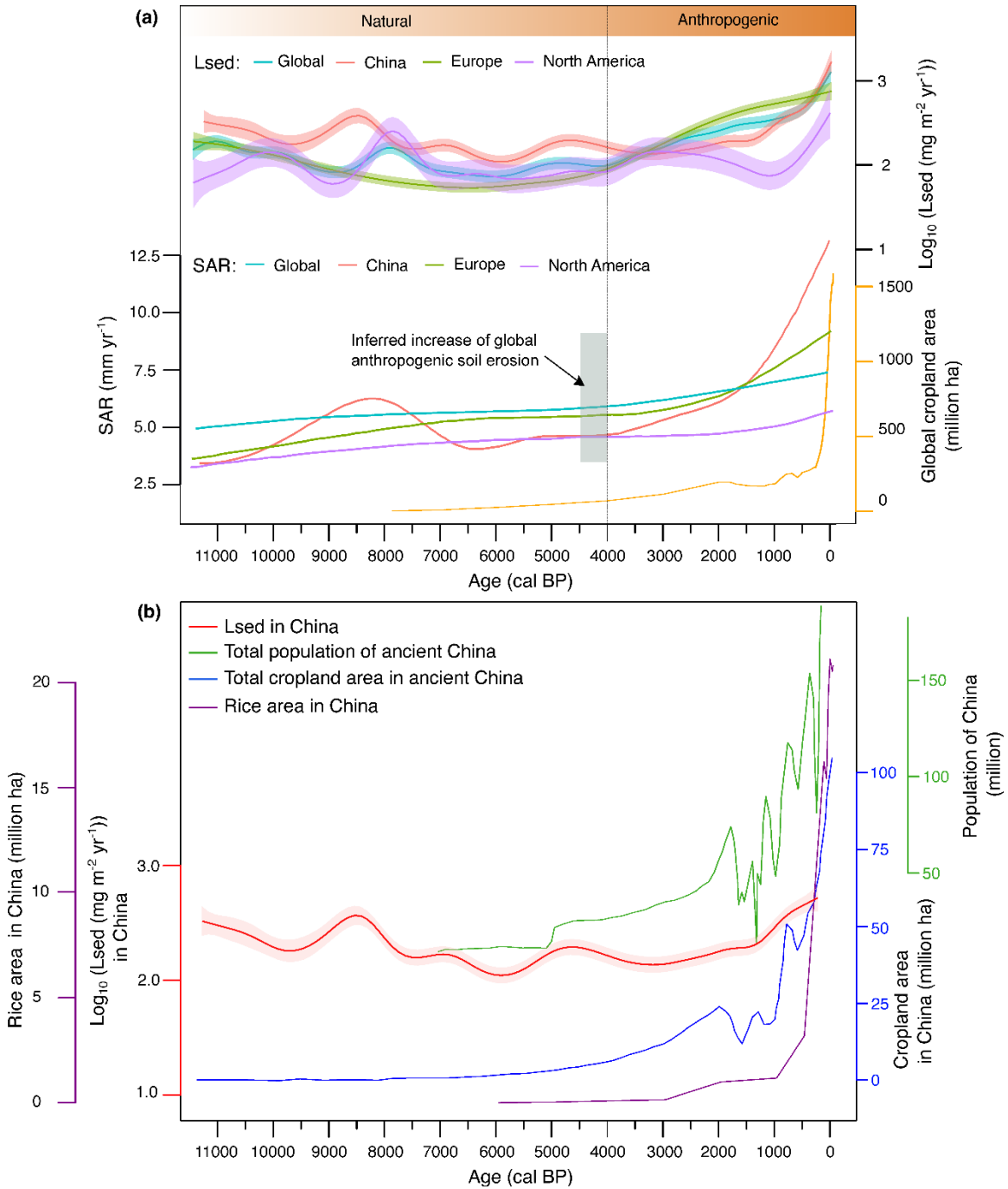
281 In Europe, the first increases in Lsed (~4500-4000 cal BP; Fig. 4a) are coincident
282 with accelerated soil erosion caused by deforestation and intensive land use
283 (Boyle et al., 2015; Moyle et al., 2021a). In North America, the notable rise in
284 sediment P burial rates occurred later than in Europe (after ~550 cal BP, Fig. 3c).
285 This record shows co-variations with enhanced rates of soil erosion in North
286 America (Fig. 4a) which was very likely attributable to European colonization
287 (Jenny et al., 2019; Kemp et al., 2020). Although elevated sediment P burial rates
288 occurred in some lakes of North America during the Early Holocene (~11,000-7500
289 cal BP), data for this period are sparse (n=133, Fig. 3c).

290 In China, the first noticeable increase in P burial rates (~2000 cal BP) was later
291 than the early record of soil erosion (Fig. 4a; Zhang et al., 2022). This can be
292 explained by the fact that most of the long-term lake P records from China selected
293 for this study are distributed in the middle and lower reaches of the Yangtze River
294 Basin (east-central China) and in southwest China (Fig. 1). During the Bronze Age
295 and early Iron Age (~4000-2000 cal BP), however, the economic center and the
296 most populated areas of China were in northern and central China (Ashley et al.,
297 2011; Li et al., 2021). It is therefore reasonable to infer that before ~2000 cal BP,
298 human disturbances in lake catchments of east-central and southwest China
299 remained relatively low (Hosner et al., 2016). Consequently, P loading from
300 croplands, through manure application and soil erosion, was probably limited. P
301 burial rates in Chinese lakes increased strongly after ~2000 cal BP, particularly
302 after ~1500 cal BP (Fig. 3a and 4), broadly coincident with increased rice
303 agriculture (mainly in southern and southwestern China; Klein Goldewijk and
304 Ramankutty, 2004) and more rapid increases in soil erosion (Zhang et al., 2022),
305 population growth (Li et al., 2009), and expansion of cropland areas in ancient
306 China (Fig. 4b; Klein Goldewijk et al., 2017). This finding indicates increasing

307 anthropogenic impacts on lake P burial after 2000-1500 cal BP, which is supported
308 by archaeological evidence documenting a large population migration from
309 northern China to central-eastern China after the Sui Dynasty (~1500-1400 cal BP;
310 Li et al., 2021). China has a long history of using P-rich animal manure and human
311 excreta as fertilizer (dating back to ~4000-5000 years ago; Ashley et al., 2011).
312 Therefore, it is probable that anthropogenic land-use and soil erosion intensified
313 across the country around 4000 years ago (Fig. 4a; Zhang et al., 2022). Although
314 the site coverage does not represent the whole continent (Fig. 1a), initial
315 anthropogenic impacts on the P cycle in China may also have occurred early in
316 the Late Holocene, ~4000 cal BP in regions with dense Bronze Age and Iron Age
317 populations. As predicted, this mirrors the pattern of early P burial increases seen
318 across Europe. However, further investigations, with more lake-sediment P
319 records over multi-millennial intervals across China, are needed to better
320 support this argument.

321 The Holocene record of soil erosion intensity in South America is not available, yet
322 the modelled P burial rates increased continuously over time during the Holocene
323 (Fig. 3d). Nevertheless, relatively high Lsed values during pre-industrial times
324 coincide with early-anthropogenic land use during agricultural expansion (5000 BP
325 to 1500 CE) and the colonial period (1500 to 1800s CE) in South America (Armesto
326 et al., 2010). This phenomenon implies detectable early-anthropogenic impacts on
327 terrestrial P cycling in South America.

328



329

330 Fig. 4. (a) Comparison of Lsed (GAM-fitted trends of 100-yr binned means), soil erosion
 331 intensity (reconstructed from lake sediment accumulation rates, SAR) at global (for 632
 332 sites, Jenny et al., 2019, SAR data n=3980) and continental levels (Jenny et al., 2019;
 333 Zhang et al., 2022), and global cropland area during the Holocene (Klein Goldewijk et al.,
 334 2017); the global synthesis of Lsed values (this study) is represented by 108 lakes; the
 335 rectangle and vertical grey line indicate the timing of early increases in anthropogenic soil

336 erosion globally (Jenny et al., 2019). (b) Comparisons of the GAM-fitted trend of Lsed
337 values in Chinese lakes between 11,500 cal BP and 150 cal BP with estimated population
338 (Li et al., 2009), total cropland area (Klein Goldewijk et al., 2017), and rice area estimates
339 (Li et al., 2009). Note that in (a) and (b) the dataset of Lsed is \log_{10} -transformed and the
340 fits of Lsed are the result of GAM with REML-based smoothness, with 95% confidence
341 intervals on predicted means (shaded envelopes).

342 3.2. Early anthropogenic impacts on global lake P burial rates since the Late 343 Holocene

344 The global pattern of Lsed values (Fig. 2a) is biased towards Europe and China
345 (Fig. 3a, b) because these areas represent a large portion of sites in our
346 compilation (69%; Fig. 1). Nonetheless, the general trend for increasing global
347 Lsed values since ~4500-4000 cal BP (Fig. 4a) tracks early increases in global soil
348 erosion intensity (proxy of SAR; Fig. 4a; Jenny et al., 2019), global cropland area
349 (Fig. 4a; Li et al., 2009), and deforestation in lake watersheds at global levels (Mottl
350 et al., 2021). A GAM fit to global soil erosion intensity (Jenny et al., 2019) explains
351 ~86 % of the variance in global average Lsed values from the Early Holocene to
352 1850 CE ($R^2_{\text{adj}} = 0.85$). The predictor of soil erosion intensity is significant (p-value
353 $< 2e-16$), whereas the contributions of climate variables (air temperature and
354 atmospheric CO₂) and global cropland areas to Lsed values are not significant (p-
355 values are 0.73, 0.55, and 0.18, respectively). Therefore, statistical analyses
356 support the inference that anthropogenic landscape disturbance and associated
357 intensified soil erosion was the leading driver for intensified global lake P burial
358 rates in pre-industrial periods.

359 The mean global Lsed between ~4000 and 100 cal BP was significantly higher
360 than (almost double) that before ~4000 cal BP (Fig. 5), which indicates that global
361 P input to freshwater since the beginning of the Late Holocene increased over
362 natural background levels. Whereas anthropogenic disruption of the global P cycle
363 since the 20th century is well documented (Liu et al., 2016; Yuan et al., 2018;
364 Scholz and Wellmer, 2019), only a handful of studies of European lakes have
365 recognized early anthropogenic impacts (Boyle et al., 2015; Klamt et al., 2021;
366 Moyle et al., 2021a). Our results reveal that human activities began to interfere

367 with the global terrestrial P cycle from the Middle-Late Holocene, suggesting this
368 pattern is spatially much wider than previously recognized. The profound early
369 anthropogenic impact on the P cycle is particularly observed in Europe and China,
370 where there are long histories of agricultural land-use and landscape disturbance
371 (Klein Goldewijk et al., 2017). Our findings support those of Moyle et al. (2021a)
372 who revealed substantial impacts of human activities on terrestrial P cycling from
373 ~6000 cal BP in lowland Europe.

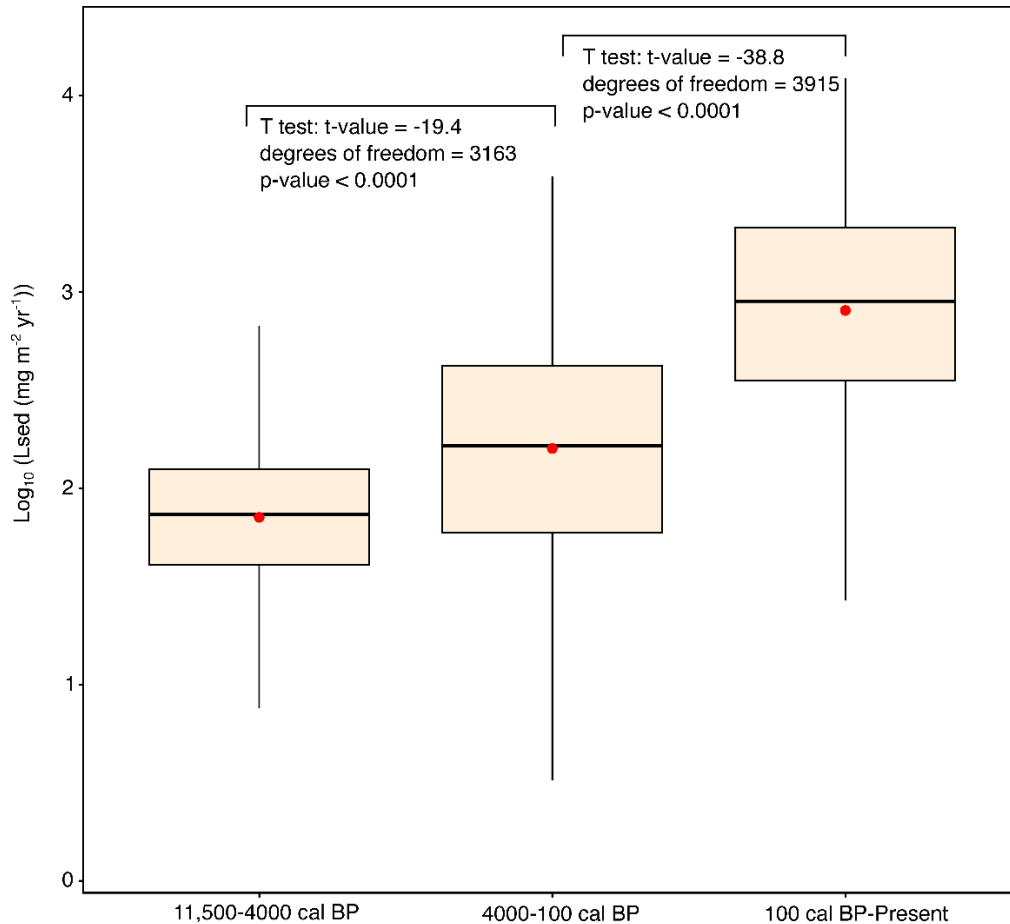
374 3.3. Global and continent-scale lake P burial rates in recent times

375 Although continental increases in lake P loading started millennia ago, the most
376 substantial increase in lake P loading occurred in the last 100 to 200 years (Fig.
377 2a; Fig. S2), coinciding with intensive farming practices and industrialization. Over
378 this period global P burial has increased consistently through time (Fig. 6). The
379 substantial increase in anthropogenic P loading over the past century has
380 enhanced P concentrations in both global lake waters and lake sediments
381 (Sharpley et al., 2013; Moyle et al., 2021a). This study shows that lake P burial
382 records on a global scale match well with the historical use of mineral P fertilizers
383 from the late 19th century onward (Fig. S3a, b), and confirms the effects of
384 anthropogenic P use on lake P burial rates on a decadal timescale.

385 Consistent with the global average, lake sediment P accumulation records from all
386 continents show systematic increases from 1850 CE to 1950 CE (Fig. 6). However,
387 since 1950 CE, China and Europe show an accelerating trend, whereas the
388 records of North America and South America have declined, and Africa has
389 increased steadily. These distinct patterns of P sequestration across the continents
390 are likely to be a consequence of different patterns of variable landscape history
391 (Moyle et al. 2021a) and/or lake morphological and hydrological factors, though
392 sampling bias i.e., small sample sizes (n= 68 for Africa and n=34 for South America)
393 may also explain the pattern. China has the highest mean lake P burial rate (~2000
394 mg P m⁻² year⁻¹; Fig. 6), which may reflect high P fertilizer use and runoff. In China,
395 the steady increase in Lsed values since the 1950s mirrors the intensified P
396 fertilizer input and the calculated P loss into freshwaters (Fig. S3a, c). This result

397 is consistent with previous studies that showed intense P fertilizer input constituted
398 the highest contribution to sediment P enrichments in China over the past century
399 (Li et al., 2015; Lu and Tian, 2016).

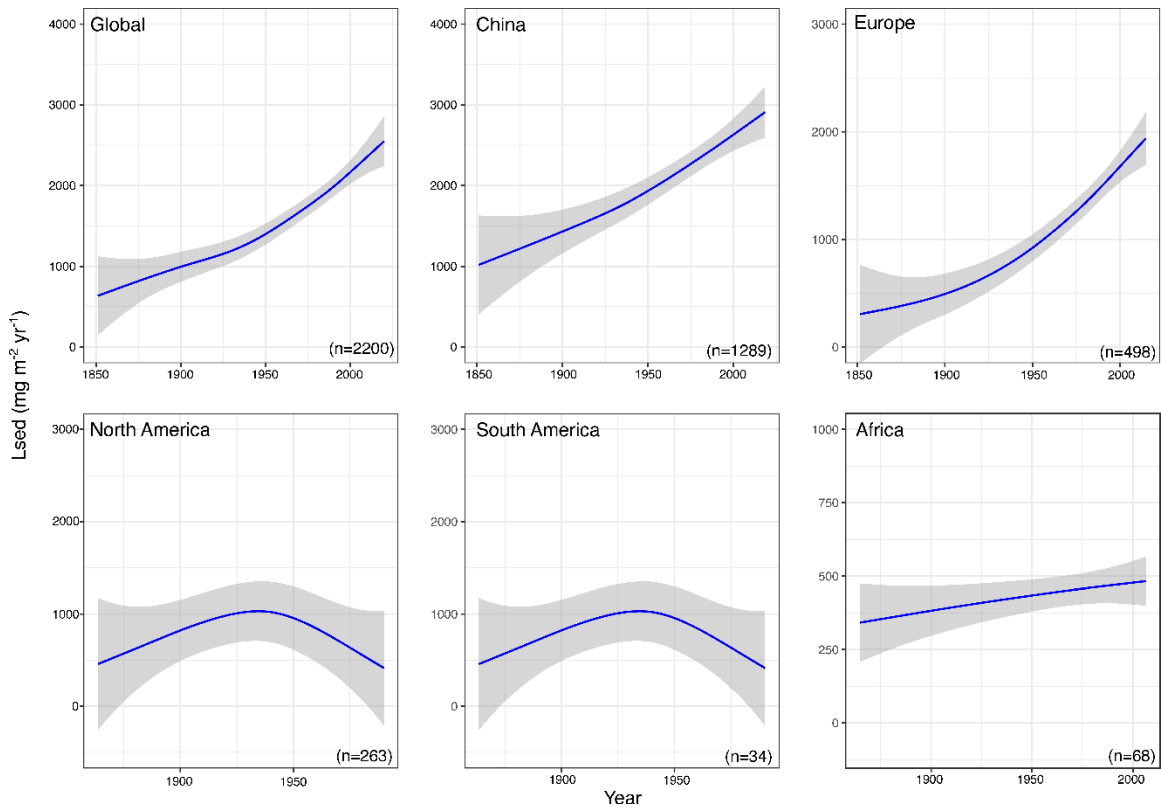
400



401

402 Fig. 5. Boxplots showing the global synthesis of Lsed from three time-intervals: Early and
403 Middle Holocene (11,500 to 4000 cal BP), Late Holocene (4000 to 100 cal BP), and recent
404 times (from 100 cal BP to present). The red dot and the black horizontal line in each
405 boxplot indicate mean and median value of the interval, respectively. The dataset of Lsed
406 was log₁₀-transformed.

407



408

409 Fig. 6. Comparative Lsed records for selected continents since 1850 CE as GAM curves
 410 with REML smoothness selection ($k=10$) and shaded 95% confidence intervals.

411

412 3.4. Estimates of total global P sequestration rates by lake sediments

413 Our dataset enables estimates of modern and Holocene global P sequestration
 414 rates in lake sediments (Table S2), which provides insights into previously poorly
 415 constrained long-term global transport and deposition of P. The global average
 416 lake sediment P sequestration rate in the Early and Middle Holocene (before
 417 ~ 4000 cal BP), i.e., with limited human impacts, is ~ 0.16 Tg P yr^{-1} . This doubled
 418 between ~ 4000 cal BP and 1850 CE to an average of ~ 0.32 Tg P yr^{-1} (Table S2),
 419 and increased ten-fold after 1850 CE to an average of ~ 1.54 Tg P yr^{-1} . This result
 420 emphasizes the extent to which human activity has caused global lake P inputs
 421 and sequestration to accelerate above the natural background. Our estimate of the
 422 global lake sediment P sequestration rate of ~ 1.54 Tg P yr^{-1} for recent times is of
 423 the same order of magnitude as the value of P retention in freshwaters (5.4 ± 3.2

424 Tg P yr⁻¹) reported by Yuan et al. (2018). Although this study is the first global
425 review of long-term lake P records, and therefore represents the best estimates of
426 lake P sequestration to date, we speculate that our estimate of ~1.54 Tg P yr⁻¹
427 likely underestimates current rates of global P sequestration in lakes, considering
428 the number of lakes represented here and the widely reported increases in P
429 supply over the period 1850 CE to present. Burial in lake sediments represents
430 one, if not the most important, mechanism for retaining P in freshwater systems as
431 a whole.

432 Quantifying the fate of P in freshwater ecosystems is important for validating ESMs
433 that attempt to model biogeochemical cycles (Lacroix et al., 2020). Yet most global
434 ESMs do not account for human impacts on terrestrial and freshwater P cycles
435 during the Holocene (Reed et al., 2015). Missing or low-resolution long records are
436 an inherent problem that precludes accurate estimation of the global lake sediment
437 P sink throughout most of the Holocene period. Here, we provide a conservative
438 estimate of ~2686 Tg P for the global lake sediment P sink (in all biomes) over the
439 Holocene (Table S2). As not all biomes are represented in this study, it is not
440 possible to make conclusive statements on the contribution of the different biomes
441 to the global P sink, however this study represents the best estimate of the global
442 Holocene lake sediment P sink to date. This sequestered P pool is permanently
443 stored by lake sediments, removing it from the P cycle of terrestrial ecosystems.
444 This significant P sink has not been considered in the framework of ESMs on
445 centennial to millennial timescales. Incorporating global lake sediment P
446 sequestration rates and total P sinks during the Holocene (~2686 Tg P) into the
447 framework of ESMs will improve our understanding of P cycling in the environment
448 and its responses to global climate change.

449 Our database with long-term records is biased towards, or over-represents, the
450 temperate and boreal continents (Fig. 1a) in the Northern Hemisphere. The
451 Southern Hemisphere and high latitudes of Europe, Asia, and North America are
452 underrepresented, leading to a significant data gap. This highlights the importance
453 of a broad geographic distribution of lake P records and illustrates the need to
454 target underrepresented areas in future studies. Our study also supports previous

455 findings about the imbalanced distribution of paleolimnological study sites (Smil,
456 2000; Mendonça et al., 2017; Dubois et al., 2018; Escobar et al., 2020). The lack
457 of data from some of the major lakes in these underrepresented areas also affects
458 our calculated global lake P sink, however this value still represents the most
459 comprehensive global estimate to date. Future research should be directed
460 towards improving this dataset with more well-dated and long-term P records from
461 underrepresented areas.

462 **4. Conclusions**

463 Using lake sediment P records from 108 lakes across the globe, we present the
464 most comprehensive study of anthropogenic modification of P sequestration in
465 lake sediments over the Holocene. Consistent with the widely recognized human
466 perturbation of the global P cycle from the industrial period (1850 CE) to the
467 present day, we show the highest lake sediment P burial rates occurred over the
468 last 100-200 years, coinciding with an expansion in population, increased sewage
469 inputs, agricultural intensification, and the use of chemical fertilizers. This
470 highlights a significant perturbation of the natural global P cycle during this period.
471 Crucially, our results reveal that human activity has impacted the global terrestrial
472 P cycle from the Late Holocene (~4000 cal BP), showing that not only do
473 anthropogenic impacts on the global P cycle extend over millennial timescales, but
474 that this pattern is spatially much wider than previously recognized. We find the
475 timings of early increases in P mobilization differed among Europe, Asia [China],
476 and North America, largely related to different land-use practices.

477 Combining the lake sediment records from our global dataset, we provide the
478 estimates of the total Holocene P sequestration in lake sediments (~2686 Tg P),
479 representing a substantial global P sink. Incorporating this value into the
480 framework of ESMs will improve our understanding of long-term P cycling and its
481 responses to global climate change. However, despite being the most
482 comprehensive study on long-term global lake sediment P burial to date, our
483 database is biased towards the Northern Hemisphere. We therefore reiterate the

484 need for future research to be directed towards collecting well-dated and long-term
485 lake sediment P records from underrepresented areas.

486 **CRedit authorship contribution statement**

487 **Luyao Tu:** Conceptualization, Methodology, Formal analysis, Writing-Original
488 Draft, Visualization, Data Curation, Funding acquisition. **Madeleine Moyle:**
489 Methodology, Validation, Writing-Review & Editing. **John F. Boyle:** Methodology,
490 Validation, Writing-Review & Editing. **Paul D. Zander:** Methodology, Validation,
491 Writing-Review & Editing. **Tao Huang:** Validation, Visualization, Writing-Review &
492 Editing. **Lize Meng:** Resources, Writing-Review & Editing. **Changchun Huang:**
493 Supervision, Validation, Writing-Review & Editing. **Martin Grosjean:** Methodology,
494 Supervision, Validation, Funding acquisition, Writing-Review & Editing. **Xin Zhou:**
495 Supervision, Funding acquisition, Validation, Writing-Review & Editing.

496 **Declaration of Competing Interest**

497 The authors declare that they have no competing financial interests or personal
498 relationships that could have appeared to influence the work reported in this paper.

499 **Supplementary Information**

500 Supplementary information will be available in the online version of the paper.

501 **Data availability**

502 The data will be available at Mendeley Data Repository.

503 **Acknowledgements**

504 This work was supported by the Swiss National Science Foundation (grant number
505 200020_204220), National Science Foundation of China (grant number
506 211410B32208), Natural Science Research of Jiangsu Higher Education

507 Institutions of China (grant number 211410B52211), the National Key R&D
508 Program of China (grant number 2022YFF0801101), and a research grant from
509 Nanjing Normal University. We thank the authors who contributed their data for the
510 purpose of this work. We thank Dr. Mark Brenner and an anonymous reviewer for
511 their constructive and thoughtful comments.

512 **References**

- 513 Alewell, C., Ringeval, B., Ballabio, C., Robinson, D.A., Panagos, P., and Borrelli, P., 2020.
514 Global phosphorus shortage will be aggravated by soil erosion. *Nat. Commun.*
515 11,1–12. <https://doi.org/10.1038/s41467-020-18326-7>.
- 516 Anderson, N.J., Heathcote, A.J., Engstrom, D.R., and Globocarb data contributors, 2020.
517 Anthropogenic alteration of nutrient supply increases the global freshwater carbon
518 sink *Sci. Adv.* 6, eaaw2145. DOI: 10.1126/sciadv.aaw2145.
- 519 Armesto, J.J., Manuschevich, D., Mora, A., Smith-Ramirez, C., Rozzi, R., Abarzúa, A.M.,
520 and Marquet, P.A., 2010. From the Holocene to the Anthropocene: A historical
521 framework for land cover change in southwestern South America in the past 15,000
522 years. *Land Use Policy* 27,148–160. <https://doi.org/10.1016/j.landusepol.2009.07.006>.
- 523 Ashley, K., Cordell, D., and Mavinic, D., 2011. A brief history of phosphorus: from the
524 philosopher's stone to nutrient recovery and reuse. *Chemosphere* 84, 737–746.
525 <https://doi.org/10.1016/j.chemosphere.2011.03.001>.
- 526 Avnimelech, Y., Ritvo, G., Meijer, L.E., and Kochba, M., 2001. Water content, organic
527 carbon and dry bulk density in flooded sediments. *Aquacult. Eng.* 25, 25–33.
528 [https://doi.org/10.1016/S0144-8609\(01\)00068-1](https://doi.org/10.1016/S0144-8609(01)00068-1).
- 529 Bhattacharya, R., Lin, S.G., and Basu, N.B., 2022. Windows into the past: lake sediment
530 phosphorus trajectories act as integrated archives of watershed disturbance legacies
531 over centennial scales. *Environ. Res. Lett.* 17, 034005. DOI 10.1088/1748-
532 9326/ac4cf3.
- 533 Boyle, J.F., 2002. Inorganic Geochemical Methods in Palaeolimnology. In: Last, M., Smol,
534 J. (eds) *Tracking Environmental Change Using Lake Sediments. Developments in*
535 *Paleoenvironmental Research*, Vol. 2. Springer, Dordrecht.

- 536 Boyle, J., Chiverrell, R., Plater, A., Thrasher, I., Bradshaw, E., Birks, H., and Birks, J.,
537 2013. Soil mineral depletion drives early Holocene lake acidification. *Geology* 41,
538 415–418.
- 539 Boyle, J.F., Chiverrell, R.C., Davies, H., and Alderson, D.M., 2015. An approach to
540 modelling the impact of prehistoric farming on Holocene landscape phosphorus
541 dynamics. *The Holocene* 25, 203–214. <https://doi.org/10.1177/0959683614556381>.
- 542 Chen, M. P. and Graedel, T. E., 2016. A half-century of global phosphorus flows, stocks,
543 production, consumption, recycling, and environmental impacts. *Glob. Environ.*
544 *Change* 36, 139–152. <https://doi.org/10.1016/j.gloenvcha.2015.12.005>.
- 545 Cordell, D., Drangert, J., and White, S., 2009. The story of phosphorus: global food
546 security and food for thought. *Glob. Environ. Change* 19, 292–305.
547 <https://doi.org/10.1016/j.gloenvcha.2008.10.009>.
- 548 Dubois, N., Saulnier-Talbot, É., Mills, K., Gell, P., Battarbee, R., Bennion, H., Chawchai,
549 S., Dong, X., Francus, P., Flower, R., and Gomes, D.F., 2018. First human impacts
550 and responses of aquatic systems: A review of palaeolimnological records from
551 around the world. *Anthr. Rev.* 5, 28–68. <https://doi.org/10.1177/2053019617740365>
- 552 Escobar, J., Serna, Y., Hoyos, N., Velez, M.I., and Correa-Metrio, A., 2020. Why we need
553 more paleolimnology studies in the tropics. *J. Paleolimnol.* 64, 47–53.
554 <https://doi.org/10.1007/s10933-020-00120-6>.
- 555 Klein Goldewijk, K. and Ramankutty, N., 2004. Land cover change over the last three
556 centuries due to human activities: The availability of new global data sets. *GeoJournal*
557 61, 335–344. <https://doi.org/10.1007/s10708-004-5050-z>.
- 558 Hosner, D., Wagner, M., Tarasov, P.E., Chen, X., and Leipe, C., 2016. Spatiotemporal
559 distribution patterns of archaeological sites in China during the Neolithic and Bronze
560 Age: An overview. *The Holocene* 26, 1576–1593.
561 <https://doi.org/10.1177/0959683616641743>.
- 562 Hosner, D., Wagner, M., Tarasov, P.E., Chen, X., and Leipe, C., 2016. Spatiotemporal
563 distribution patterns of archaeological sites in China during the Neolithic and Bronze
564 Age: An overview. *The Holocene* 26, 1576–1593.
565 <https://doi.org/10.1177/0959683616641743>.

566 Hurtado, S.I., Zaninelli, P.G., and Agosta, E.A., 2020. A multi-breakpoint methodology to
567 detect changes in climatic time series. An application to wet season precipitation in
568 subtropical Argentina. *Atmos. Res.* 241, 104955.
569 <https://doi.org/10.1016/j.atmosres.2020.104955>.

570 Jenny, J.P., Koirala, S., Gregory-Eaves, I., Francus, P., Niemann, C., Ahrens, B., Brovkin,
571 V., Baud, A., Ojala, A.E., Normandeau, A., and Zolitschka, B., 2019. Human and
572 climate global-scale imprint on sediment transfer during the Holocene. *Proc. Natl.*
573 *Acad. Sci. U.S.A.* 16, 22972–22976. <https://doi.org/10.1073/pnas.1908179116>.

574 Kemp, D.B., Sadler, P.M., and Vanacker, V., 2020. The human impact on North American
575 erosion, sediment transfer, and storage in a geologic context. *Nat. Commun.* 11, 1–9.
576 <https://doi.org/10.1038/s41467-020-19744-3>.

577 Klamt, A.M., Poulsen, S.P., Odgaard, B.V., Hübener, T., McGowan, S., Jensen, H.S., and
578 Reitzel, K., 2021. Holocene lake phosphorus species and primary producers reflect
579 catchment processes in a small, temperate lake. *Ecol. Monogr.* 91, e01455.
580 <https://doi.org/10.1002/ecm.1455>.

581 Klein Goldewijk, K., Beusen, A., Doelman, J., and Stehfest, E., 2017. Anthropogenic land
582 use estimates for the Holocene–HYDE 3.2. *Earth Syst. Sci. Data* 9, 927–953.
583 <https://doi.org/10.17026/dans-25g-gez3>.

584 Klein, K. and Ramankutty, N., 2004. Land cover change over the last three centuries due
585 to human activities: The availability of new global data sets. *GeoJournal* 61, 335–344.
586 <https://doi.org/10.1007/s10708-004-5050-z>.

587 Lacroix, F., Ilyina, T., and Hartmann, J., 2020. Oceanic CO₂ outgassing and biological
588 production hotspots induced by pre-industrial river loads of nutrients and carbon in a
589 global modeling approach. *Biogeosciences*, 17, 55–88. <https://doi.org/10.5194/bg-17-55-2020>.

591 Li, H., Liu, Z., James, N., Li, X., Hu, Z., Shi, H., Sun, L., Lu, Y., and Jia, X., 2021.
592 Agricultural transformations and its influential factors revealed by archaeobotanical
593 evidence in Holocene in Jiangsu Province, eastern China. *Front. Earth Sci.* 9, 387.
594 <https://doi.org/10.3389/feart.2021.661684>.

595 Li, H., Liu, J., Li, G., Shen, J., Bergström, L., and Zhang, F., 2015. Past, present, and
596 future use of phosphorus in Chinese agriculture and its influence on phosphorus
597 losses. *Ambio* 44, 274–285. <https://doi.org/10.1007/s13280-015-0633-0>.

598 Li, X., Dodson, J., Zhou, J., and Zhou, X., 2009. Increases of population and expansion of
599 rice agriculture in Asia, and anthropogenic methane emissions since 5000 BP. *Quat.*
600 *Int.* 202, 41–50. <https://doi.org/10.1016/j.quaint.2008.02.009>.

601 Liu, X., Sheng, H., Jiang, S., Yuan, Z., Zhang, C., and Elser, J.J., 2016. Intensification of
602 phosphorus cycling in China since the 1600s. *Proc. Natl. Acad. Sci. U.S.A* 113, 2609–
603 2614. <https://doi.org/10.1073/pnas.1519554113>.

604 Lu, C. and Tian, H., 2016. Global nitrogen and phosphorus fertilizer use for agriculture
605 production in the past half century: shifted hot spots and nutrient imbalance. *Earth*
606 *Syst. Sci. Data Discuss.* 9, 1–33. <https://doi.org/10.5194/essd-9-181-2017>.

607 MarcFott, S. A., Shakun, J. D., Clark, P. U., and Mix, A. C., 2013. A reconstruction of
608 continental and global temperature for the past 11,300 years. *Science* 339, 1198–
609 1201. <https://doi.org/10.1126/science.1228026>.

610 McCormac, F., Hogg, A., Blackwell, P., Buck, C., Higham, T., and Reimer, P., 2004.
611 Shcal04 Southern Hemisphere Calibration, 0–11.0 Cal Kyr BP. *Radiocarbon* 46,
612 1087–1092. <https://doi.org/10.1017/S0033822200033014>.

613 Mendonça, R., Müller, R.A., Clow, D., Verpoorter, C., Raymond, P., Tranvik, L.J., and
614 Sobek, S., 2017. Organic carbon burial in global lakes and reservoirs. *Nat. Commun.*
615 8,1–7. <https://doi.org/10.1038/s41467-017-01789-6>.

616 Mottl, O., Flantua, S.G., Bhatta, K.P., Felde, V.A., Giesecke, T., Goring, S., Grimm, E.C.,
617 Haberle, S., Hooghiemstra, H., Ivory, S., and Kuneš, P., 2021. Global acceleration in
618 rates of vegetation change over the past 18,000 years. *Science* 372, 860–864.
619 <https://doi.org/10.1126/science.abg1685>.

620 Moyle, M. and Boyle, J.F., 2021. A method for reconstructing past lake water phosphorus
621 concentrations using sediment geochemical records. *J. Paleolimnol.* 65, 461–478.
622 <https://doi.org/10.1007/s10933-021-00174-0>.

623 Moyle, M., Boyle, J.F., and Chiverrell, R.C., 2021a. Towards a history of Holocene P
624 dynamics for the Northern Hemisphere using lake sediment geochemical records.
625 *Biogeosciences* 18, 5609–5638. <https://doi.org/10.5194/bg-18-5609-2021>.

626 Moyle, M., Boyle, J.F., and Chiverrell, R.C., 2021b. Holocene records of Sediment Inferred
627 [lake water] Total Phosphorus concentration (SI-TP) and landscape phosphorus
628 yield. [Data Collection]. <https://doi.org/10.17638/datacat.liverpool.ac.uk/1272>.

629 Olson, D.M., Dinerstein, E., Wikramanayake, E.D., Burgess, N.D., Powell, G.V.,
630 Underwood, E.C., D'amico, J.A., Itoua, I., Strand, H.E., Morrison, J.C., and Loucks,
631 C.J., 2001. Terrestrial Ecocontinents of the World: A New Map of Life on Earth A new
632 global map of terrestrial ecocontinents provides an innovative tool for conserving
633 biodiversity. *BioScience* 51, 933–938. [https://doi.org/10.1641/0006-](https://doi.org/10.1641/0006-3568(2001)051[0933:TEOTWA]2.0.CO;2)
634 [3568\(2001\)051\[0933:TEOTWA\]2.0.CO;2](https://doi.org/10.1641/0006-3568(2001)051[0933:TEOTWA]2.0.CO;2).

635 Ramsey C B., 2009. Bayesian analysis of radiocarbon dates. *Radiocarbon* 51, 337–360.
636 <https://doi.org/10.1017/S0033822200033865>.

637 Reed, S.C., Yang, X., and Thornton, P.E., 2015. Incorporating phosphorus cycling into
638 global modeling efforts: a worthwhile, tractable endeavor. *New Phytologist* 208, 324-
639 329. <https://doi.org/10.1111/nph.13521>.

640 Reimer, P.J., Austin, W.E., Bard, E., Bayliss, A., Blackwell, P.G., Ramsey, C.B., Butzin,
641 M., Cheng, H., Edwards, R.L., Friedrich, M. and Grootes, P.M., 2020. The IntCal20
642 Northern Hemisphere radiocarbon age calibration curve (0–55 cal kBP). *Radiocarbon*
643 62, 725–757. <https://doi.org/10.1017/RDC.2020.41>.

644 R Core Team, 2021. R: A Language and Environment for Statistical Computing, available
645 at: <https://www.r-project.org/> (last access: 15 July 2021)

646 Ruttenberg, K. C., 2003. The Global Phosphorus Cycle. In: Schlesinger, W. H. (eds)
647 *Treatise in Geochemistry*, Vol. 8. Elsevier. [https://doi.org/10.1016/B0-08-043751-](https://doi.org/10.1016/B0-08-043751-6/08153-6)
648 [6/08153-6](https://doi.org/10.1016/B0-08-043751-6/08153-6).

649 Scholz, R.W. and Wellmer, F.W., 2019. Cycling and Anthropogenic Use of Phosphorus in
650 the 21st Century: Geoscientific and Geosocial Foundations of Agriculture. *Better*
651 *Crops with Plant Food*, 103, 9–12. <http://doi.org/10.24047/BC103xx>.

652 Scholtysik, G., Goldhammer, T., Arz, H.W., Moros, M., Littke, R., and Hupfer, M., 2022.
653 Geochemical focusing and burial of sedimentary iron, manganese, and phosphorus
654 during lake eutrophication. *Limnol. Oceanogr.* 67, 768–783.
655 <https://doi.org/10.1002/lno.12019>.

656 Sharpley, A., Jarvie, H.P., Buda, A., May, L., Spears, B., and Kleinman, P., 2013.
657 Phosphorus legacy: overcoming the effects of past management practices to mitigate
658 future water quality impairment. *J. Environ. Qual.* 42, 1308–1326.
659 <https://doi.org/10.2134/jeq2013.03.0098>.

660 Simpson, G.L., 2018. Modelling palaeoecological time series using generalised additive
661 models. *Front. Ecol. Evol.* 6, 149. <https://doi.org/10.3389/fevo.2018.00149>.

662 Smil, V., 2000. Phosphorus in the environment: natural flows and human
663 interferences. *Annu. Rev. Environ. Resour.* 25, 53–88.
664 <https://doi.org/10.1146/annurev.energy.25.1.53>.

665 Steffen, W., Richardson, K., Rockström, J., Cornell, S.E., Fetzer, I., Bennett, E.M., Biggs,
666 R., Carpenter, S.R., De Vries, W., De Wit, C.A., and Folke, C., 2015. Planetary
667 boundaries: Guiding human development on a changing planet. *Science* 347,
668 1259855. <https://doi.org/10.1126/science.1259855>.

669 Wang, M., Houlton, B.Z., Wang, S., Ren, C., van Grinsven, H.J., Chen, D., Xu, J., and Gu,
670 B., 2021. Human-caused increases in reactive nitrogen burial in sediment of global
671 lakes. *The Innovation* 2, 100158. <https://doi.org/10.1016/j.xinn.2021.100158>.

672 Waters, C.N., Zalasiewicz, J., Summerhayes, C., Barnosky, A.D., Poirier, C., Gałuszka,
673 A., Cearreta, A., Edgeworth, M., Ellis, E.C., Ellis, M., and Jeandel, C., 2016. The
674 Anthropocene is functionally and stratigraphically distinct from the Holocene. *Science*
675 351, aad2622. <https://doi.org/10.1126/science.aad2622>.

676 Wood, S., 2017. *Generalized additive models: an introduction with R*, CRC press, Boca
677 Raton, FL, 496. <https://doi.org/10.1201/9781315370279>.

678 Yuan, Z., Jiang, S., Sheng, H., Liu, X., Hua, H., Liu, X., and Zhang, Y., 2018. Human
679 perturbation of the global phosphorus cycle: changes and consequences. *Environ. Sci.*
680 *Technol.* 52, 2438–2450. <https://doi.org/10.1021/acs.est.7b03910>.

681 Zhang, F., Li, S., Sun, C., Li, W., Zhao, X., Chen, Z., Nie, T., Chen, Y., and Li, X., 2022.
682 Human Impacts Overwhelmed Hydroclimate Control of Soil Erosion in China 5,000
683 Years Ago. *Geophys. Res. Lett.* 49, e2021GL096983.
684 <https://doi.org/10.1029/2021GL096983>.